Received: 25 November 2021 | Revised: 8 April 2022 | Accepted: 11 April 2022

DOI: 10.1096/fj.202101816RR

THE FASEB JOURNAL

RESEARCH ARTICLE

Ablation of uncoupling protein 3 affects interrelated factors leading to lipolysis and insulin resistance in visceral white adipose tissue

Alessandra Gentile[1] | **Nunzia Magnacca**[1] | **Rita de Matteis**[2] | **Maria Moreno**[3] | **Federica Cioffi**[3] | **Antonia Giacco**[3] | **Antonia Lanni**[4] | **Pieter de Lange**[4] | **Rosalba Senese**[4] | **Fernando Goglia**[3] | **Elena Silvestri**[3] | **Assunta Lombardi**[1]

[1]Department of Biology, University of Naples Federico II, Naples, Italy

[2]Department of Biomolecular Sciences, University of Urbino Carlo Bo, Urbino, Italy

[3]Department of Science and Technology, University of Sannio, Benevento, Italy

[4]Department of Environmental, Biological and Pharmaceutical Sciences and Technologies, University of Campania Luigi Vanvitelli, Caserta, Italy

Correspondence
Assunta Lombardi, Department of Biology, University of Naples Federico II, Via Cinthia 80126 Naples, Italy.
Email: assunta.lombardi@unina.it

Elena Silvestri, Department of Science and Technology, University of Sannio, Benevento, Italy.
Email: silvestri@unisannio.it

Present address
Alessandra Gentile, Department of Pharmacological and Biomolecular Sciences, University of Milan, Milano, Italy

Funding information
Università degli Studi di Napoli Federico II (UNINA); Università degli Studi di Urbino Carlo Bo (University of Urbino); University of Sannio

Abstract

The physiological role played by uncoupling protein 3 (UCP3) in white adipose tissue (WAT) has not been elucidated so far. In the present study, we evaluated the impact of the absence of the whole body UCP3 on WAT physiology in terms of ability to store triglycerides, oxidative capacity, response to insulin, inflammation, and adipokine production. Wild type (WT) and UCP3 Knockout (KO) mice housed at thermoneutrality (30°C) have been used as the animal model. Visceral gonadic WAT (gWAT) from KO mice showed an impaired capacity to store triglycerides (TG) as indicated by its lowered weight, reduced adipocyte diameter, and higher glycerol release (index of lipolysis). The absence of UCP3 reduces the maximal oxidative capacity of gWAT, increases mitochondrial free radicals, and activates ER stress. These processes are associated with increased levels of monocyte chemoattractant protein-1 and TNF-α. The response of gWAT to in vivo insulin administration, revealed by (ser473)-AKT phosphorylation, was

Abbreviations: ABHD5, α/β hydrolase domain-containing protein 5; ATGL, adipose triglyceride lipase; COX, cytochrome oxidase/complex IV activity; DCF, dichlorofluorescein; DCFH-DA, 2′,7′-dichlorodihydrofluorescin diacetate; DPPIV, dipeptidyl peptidase-4; eIF2α, eukaryotic initiation factor-2α; ER, endoplasmic reticulum; FFA, free fatty acids; GPX4, glutathione peroxidase-4; GRP78/BIP, 78-kDa glucose-regulated protein; IGFBP-1, IGF-binding protein-1; IRE-1, inositol-requiring ER-to-nucleus signaling protein 1; JNKs, c-Jun N-terminal kinases; MCP1, chemotactic protein-1; PAI-1, plasminogen activator inhibitor 1; PERK, RNA-dependent protein kinase (PKR)-like ER eukaryotic initiation factor-2 alpha kinase; PLIN-1, perilipin-1; PLIN1, Perilipin-1; ROS, reactive oxygen species; SOD2, superoxide dismutase protein-2; TGs, triglycerides; TimP-1, tissue inhibitor of metalloproteinases-1; TLR4, Toll-like receptors 4; TNF-α, tumor necrosis factor alpha; UCP3, uncoupling protein 3; UPR^{ER}, endoplasmic reticulum unfolded protein response; WAT, white adipose tissue.

Alessandra Gentile and Nunzia Magnacca contributed equally to this study.

blunted in KO mice, with a putative role played by eif2a, JNK, and inflammation. Variations in adipokine levels in the absence of UCP3 were observed, including reduced adiponectin levels both in gWAT and serum. As a whole, these data indicate an important role of UCP3 in regulating the metabolic functionality of gWAT, with its absence leading to metabolic derangement. The obtained results help to clarify some aspects of the association between metabolic disorders and low UCP3 levels.

KEYWORDS

endoplasmic reticulum, insulin resistance, lipolysis, mitochondria, uncoupling protein, white adipose tissue

1 | INTRODUCTION

Uncoupling protein 3 (UCP3) is a mitochondrial protein localized in the inner membrane and mainly expressed in striated muscles and adipose tissues. Among these, brown adipose tissue (BAT) mitochondria present the highest amount of the protein, while similar content was detected in heart, skeletal muscle, and white adipose tissue (WAT).[1] Involvement for UCP3 in mild uncoupling, fatty acid oxidation rate, and prevention of damage induced by reactive oxygen species (ROS) and lipid hydroperoxides has been proposed.[2–4]

Most studies have focused on the role played by UCP3 on the heart and skeletal muscle, while few studies have been dedicated to adipose organs. Only recently we reported that the absence of UCP3 has a profound effect on brown adipose tissue metabolism[5] and some indications also suggest that it could affect WAT physiology.[6] Indeed, when housed at thermoneutrality (30°C), UCP3 KO mice fed a standard diet, despite presenting unchanged whole-body composition compared to WT littermate (in terms of protein, lipid, and water percentage), show reduced visceral WAT mass associated with increased WAT lipolysis and ectopic lipid accumulation in lean tissues, such as liver and skeletal muscle.[5] An increase in serum free fatty acids (FFA) has been found associated with the absence of UCP3 in mice under standard housing temperature 20–24°C.[7] These data suggest that the absence of UCP3 likely compromises the ability of WAT to store triglycerides (TGs), a process central in the maintenance of the whole body's homeostasis. The regulation of WAT lipolysis occupies a key position in carbohydrates and lipids metabolism, and insulin plays the role of the conductor. Insulin significantly acts on adipose tissue by (i) stimulating glucose uptake and triglyceride synthesis (ii) suppressing triglyceride hydrolysis and release of FFA and glycerol into the circulation, and (iii) enhancing the activity of lipoprotein-lipase, responsible for the uptake and storage of blood lipoproteins in WAT. Thus, it is plausible that in UCP3 null mice a failure in WAT response to insulin could take place, also given the pieces of evidence obtained on mice[7–10] and human[11,12] indicating a role for UCP3 in protecting against insulin resistance. How the absence of UCP3 leads to WAT lipolysis and whether this reflects an impaired response of WAT to insulin is not known.

Crucial for adipocyte homeostasis is the functional bidirectional relationship between mitochondria and endoplasmic reticulum (ER) so a dysfunction on either side can severely disrupt cell homeostasis and lead to metabolic derangements, such as insulin resistance.[12] Indeed, the folding of proteins within ER is an energy-consuming process that is profoundly affected by the cell's redox state. Consequently, the inability of mitochondria to produce adequate levels of ATP and/or enhanced mitochondrial ROS production could induce ER stress and the activation of associated signaling pathways [known as unfolded protein response (UPR^{ER})], finalized to return the ER to homeostatic conditions.[13] In turn, when under stress, ER could relay calcium signals to mitochondria that other than activating mitochondrial ATP production induces ROS production, thus leading to mitochondrial dysfunction. Thereby, a vicious cycle is established and perpetuated. Accordingly, because of the ability of UCP3 to mitigate oxidative stress and to influence mitochondrial functionality,[4,5] it is possible that the absence of UCP3 could lead to ER stress. This is particularly intriguing since, in adipose tissue, mitochondrial dysfunctions and ER stress are associated with insulin resistance, inflammation, lipolysis, and adipokine production.[14]

The mechanism by which ER stress interferes with insulin receptor signaling is multifactorial[15] and different branches of UPR^{ER} seem to be involved. Notably, ER stress has recurrently been shown to induce cellular inflammation through activation of pathways involved in the regulation of inflammatory cytokines release.[16] Cytokines, produced by the adipocyte itself or by adipose

tissue-infiltrated macrophages, lead to a chronic subinflammatory state, central to the onset and/or to the progression of insulin resistance.[16] In addition, when FFA are released by lipolytic adipocytes, they may also activate Toll-like receptors 4 (TLR4) and then chemokines and cytokines release, thus amplifying insulin resistance, lipolysis, and inflammation in all WAT.[16]

Based on what was stated above and considering the role played by UCP3 in mitigating mitochondrial oxidative stress,[2–4] we investigated the possibility that in WAT the absence of UCP3 could lead to mitochondrial dysfunction, ER stress, inflammation, and insulin resistance. In addition, since ER has a fundamental role in adipokines synthesis and secretion, we also tested whether the absence of UCP3 could affect tissue and serum levels of these signaling molecules. Visceral adipose tissue, in particular the gonadic depot (gWAT), has been used throughout the study as it is of particular concern because it's a key player in metabolic derangements, much more so than subcutaneous WAT.[16–18] To fully underscore the role of UCP3, during experimentation mice were housed at thermoneutrality (30°C) since (i) a clear role of UCP3 on energy and lipid metabolism has been observed at thermoneutrality[5] (ii) standard housing temperature (20–24°C) for these rodents represents constant cold stress, that impacts research outcomes.

2 | METHODS

2.1 | Animals

UCP3 knockout (KO) Swiss black background mice were originally from the Reitman group.[19] KO mice and WT control mice (Swiss Black originally from Taconic, New York, USA) were housed at 30 ± 1°C, with a 12/12 h light-dark cycle and free access to food and water for 4 weeks. At the end of treatment, mice were anesthetized with Pentotal (30 mg/kg) and euthanized by cervical dislocation. Blood was collected, gWAT was dissected weighted, immediately processed, or frozen in nitrogen for later measurements.

To evaluate the response of gWAT to insulin, mice were fasted for 5 h, before receiving a single administration of insulin (0.5 U/Kg) or saline. 30 min after the administration mice were sacrificed.

This study was carried out in accordance with recommendations in the EU Directive 2010/63 for the Care and Use of Laboratory Animals. All animal protocols were approved by the Committee on the Ethics of Animal Experiments of the University of Naples Federico II and the Italian Minister of Health. Every effort was made to minimize animal pain and suffering.

Project number: 374/2017PR.

General reagents were of the highest available grade and were obtained from Merck-Sigma Aldrich Chemical (St. Louis, MO, USA).

2.2 | gWAT glycerol release

To evaluate the diffusion of glycerol from gWAT to the medium 50 mg of tissue were used. The tissue was incubated at 37°C for 1 h at 37°C in 250 μl of Krebs Ringer buffer (12 mM HEPES, 121 mM NaCl, 4.9 mM KCl, 1.2 mM $MgSO_4$, 0.33 mM $CaCl_2$) containing 2% FA-free bovine serum albumin (BSA) and 0.1% glucose. Incubations were performed under shaking in the absence and in the presence of isoproterenol (10 μM), and samples were gassed with 95% O_2–5% CO_2. At the end of the incubation period, an aliquot of the medium was used for the analysis of glycerol content. An absorbance-based enzyme assay for glycerol, commercially available (Free Glycerol Reagent; Merck Sigma Aldrich Chemical), was converted to fluorescence-based detection by the inclusion of the hydrogen peroxide-sensitive dye Amplex UltraRed, as reported by Clark 2009.[20]

2.3 | gWAT lysates and western blot

100 mg of gWAT were homogenized in 300 μl RIPA buffer (150 mM NaCl, 1.0% Triton X-100, 0.5% sodium deoxycholate, 0.1% SDS, 50 mM Tris, pH 8.0) supplemented with a broad-range antiprotease cocktail (Merck, Sigma-Aldrich Chemical). Homogenates were left on ice for 1 h, and then centrifuged at 17.000× *g* for 30 min, at 4°C; the resulting supernatants were collected.

Thereafter, 15 μg of adipose tissue lysates were separated by SDS-PAGE and transferred to nitrocellulose membranes in a dry blotting system (iBLOT 2, Thermo Fisher Scientific - USA). Membranes were blocked with Tris-buffered saline containing 0.1% Tween and 5% non-fat dry milk and were subsequently incubated overnight with the appropriate antibodies. After washing, filters were incubated with secondary horseradish peroxidase coupled antibody and processed for enhanced chemiluminescence detection using Excellent Chemiluminescent Substrate Kit (Elabscience USA). Signals were visualized by ChemiDoc™ XRS+ Imaging Systems (Bio-Rad Laboratories, Italy).

Primary antibodies used throughout the study were the following: anti-SOD-2 (ab 13533; abcam UK, Cambridge), anti-glutathione peroxidase 4 (GXP-4) (MAB5457 R&D system, Minneapolis USA), anti-CAT (ab 16731 abcam), cocktail of antibody used to detect CI-NDUF88, CII-SDHB,

CIII-UQCRC2, CIV-MTCO1 and CV- ATP VA subunits (oxophos ab110413, abcam), anti-perilipin-1 (PLIN-1) (ab3526 abcam), anti- ATGL (#2138 Cell Signaling Technology, Massachusetts, USA), anti eIF2alpha (L57A5, Cell Signaling), anti (ser 51) eIF2alpha phosphorylated form (D9G8, Cell Signaling), anti Akt/PKB total (#4691, Cell Signaling) and Ser 473 -phosphorylated Akt/PKB form (#9271, Cell Signaling), anti JNK (sc-7345, Santa Cruz Biotechnology, inc. Dallas, TX, USA), anti (Thr 183 and Tyr 185) JNK phosphorylated form (sc-6254, Santa Cruz Biotechnology, inc.), anti-Tumor Necrosis Factor Alpha TnFalfa (ab1793, Abcam), anti i Monocyte Chemotactic protein (MCP1) (Elabscinece E-AB-67848), anti-Calnexin (ab22595 abcam), anti GRP78-BIP (ab 108613 abcam), anti UCP3 (ab 3477, Abcam).

Protein representation was quantified by densitometry (Image Lab Software Biorad or Image J software) and normalized based on loading controls α-tubulin (ab4074, Abcam) or β actin (E-AB-20031, Elabscience) or HSP60 (GTX 110089 GeneTex).

2.4 | Histological analysis

For histological analysis, samples of gWAT were fixed by immersion in 4% v/v formaldehyde in 0.1 M phosphate buffer at 4°C, overnight. The samples were then dehydrated in ethanol, cleared, and embedded in paraffin blocks. For morphological examination, the tissues were cut into serial sections (6-μm-thick) and then were stained with hematoxylin-eosin. Sections were viewed with a Nikon Eclipse 80i light microscope (Nikon Instruments, Milan, Italy) at 20× magnification. Images were obtained with a Sony DS-5M camera connected to an ACT-2U image analyzer.

2.5 | Cytochrome oxidase activity

To detect Cytochrome oxidase activity, 100 mg of gWAT was homogenized in 1 ml of a buffer constituted by (220 mM mannitol, 70 mM sucrose, 20 mM Tris-HCl, 1 mM EDTA, 5 mM EGTA (pH 7.4)). The homogenate was centrifuged at 500× *g* and the upper-fat layer was removed. The remaining supernatant and the pellet were resuspended and re-homogenized. The samples were diluted 1:2 with the same buffer containing lubrol (1% w/vol) and then kept on ice for 30 min. Cytochrome oxidase activity was determined polarographically at 37°C by using the Oroboros 2k-Oxygraph system instrument (Innsbruck Austria). Homogenate was incubated in 2 ml of reaction medium containing 30 μM cytochrome c, 4 μM rotenone, 0.5 mM dinitrophenol, 10 mM Na-malonate, and 75 mM HEPES at pH 7.4. After about 10 min the substrate [4 mM Na ascorbate with 0.3 mM *N*,*N*,*N*′,*N*′-tetramethyl-p-phenylenediamine] was added and oxygen consumption was detected. The auto-oxidation of the substrate was evaluated in parallel measurements in the absence of homogenate.[21] Sample protein content was determined using Bio-Rad Protein Assay Dye (Bio-Rad Laboratories).

2.6 | Insulin and glucose serum levels

Insulin and glucose were detected in sera from mice under 5 h of fasting, by mouse insulin Elisa Kit (Mercodia AB, Sweden) and glucose assay kit by Merck (Sigma Aldrich), following manufacturers' indications.

2.7 | Mitochondrial ROS levels

Mitochondrial ROS content was detected in isolated mitochondria. Fragments of gWAT (500 mg) were immersed in ice-cold isolation buffer (220 mM mannitol, 70 mM sucrose, 20 mM Tris-HCl, 1 mM EDTA, 5 mM EGTA, and 1% fatty acid-free bovine serum albumin [BSA]; pH 7.4), and then homogenized in a Potter-Elvehjem homogenizer (Heidiolph Instruments, Germany). To remove fat, the homogenate was centrifuged at 10.000× *g* for 10 min at 4°C. Floating fat was removed, the pellet resuspended in the original volume and centrifuged at 700× *g* for 10 min. The resulting supernatant was centrifuged at 3000× *g* to obtain a mitochondrial pellet. Mitochondrial pellets were washed twice and resuspended in a minimal volume of isolation medium and kept on ice. Mitochondrial ROS levels were measured following the ROS-induced conversion of 2′,7′-dichlorodihydrofluorescin diacetate (DCFH-DA, nonfluorescent compound) in dichlorofluorescein (DCF, fluorescent compound) according to Driver et al. 2000.[22] In brief, 10 μg mitochondrial proteins in 200 μl of monobasic phosphate buffer 0.1 M, pH 7.4, were incubated for 15 min with 10 μM DCFH-DA. Then, FeCl3 was added (final concentration 100 μM), and the mixture was incubated for 30 min. The conversion of DCFH-DA to the fluorescent product DCF was measured using a multimode microplate reader (Tecan Infinite 200 pro plate reader) with excitation and emission wavelengths of 485 and 530 nm, respectively. Background fluorescence (conversion of DCFH to DCF in the absence of mitochondria) was corrected with parallel blanks. A standard curve of DCF was used to calculate pmol DCF formed.

2.8 | Adipokines content analysis

A Proteome Profiler Mouse Adipokine Array (R&D Systems, USA) has been used for the parallel determination of the relative levels of selected mice Adipokine, by following the manufacturer's indication.

2.9 | Statistical analysis

Data are reported as mean ± SEM. Data were analyzed by a two-tailed Student's *t*-test and differences have been considered statistically significant at $p < .05$.

3 | RESULTS

3.1 | Absence of UCP3 reduces gWAT weight, adipocytes size and increases the lipolytic processes

The absence of UCP3 reduced the weight of gWAT (by 43%) as well as its contribution to the total animal weight (by 33%), while no differences were observed when considering heart, gastrocnemius, interscapular brown adipose tissue, and liver (Table 1).

In gWAT from mice under thermoneutral conditions, a UCP3-specific signal was detected in mitochondria from WT samples but not in KO ones (Figure 1A). Histological analysis of gWAT from WT and KO mice indicated that adipocytes size was approximately halved in KO mice compared to the WT control ones (Figure 1B,C). Moreover, in gWAT from KO mice, an enhanced lipolytic capacity was observed, as revealed by increased glycerol release (Figure 1D), as well as by the reduction in Perilipin-1 (PLIN1) (−90% vs. WT) (Figure 1E), a protein fundamental in lipolysis process. No changes in adipose triglycerides lipase (ATGL) protein levels were observed between the WT and KO mice (Figure 1F).

TABLE 1 Body weight, WAT weight, and contribution of tissues to the whole body weight detected in WT and KO mice

	WT	KO
Body weight (g)	32.3 ± 1.0	29.3 ± 1.1*
gWAT weight (g)	1.20 ± 0.08	0.68 ± 0.02*
Tissue weight/body weight * 100		
gWAT	3.68 ± 0.32	2.34 ± 0.06*
BAT	0.74 ± 0.04	0.69 ± 0.04
Heart	0.42 ± 0.02	0.43 ± 0.02
Liver	4.04 ± 0.16	4.31 ± 0.14
Gastrocnemius Skeletal muscle	0.91 ± 0.04	1.06 ± 0.06

Note: Values represent the mean ± SE of 10 different mice.

*$p < .01$ versus WT.

3.2 | Absence of UCP3 blunts AKT phosphorylation in response to in vivo insulin administration

KO mice, following 5 h fasting, displayed unchanged glucose serum (Figure 2A) and enhanced insulin (Figure 2B), thus accounting for a condition of insulin resistance. Accordingly, the response of gWAT to the in vivo administration of insulin was blunted in KO mice. In basal conditions the total level of Akt/PKB and Ser 473 -phosphorylated Akt/PKB were not significantly affected by the absence of UCP3 (Figure 2C), while the administration of insulin enhanced AKT phosphorylation, with the effect being significantly lower in KO mice Significant activation of AKT following insulin administration was observed only in WT mice, as revealed by the ratio pAKT/AKT (Figure 2C).

3.3 | Absence of UCP3 influences gWAT mitochondrial functionality, oxidative stress, and enzymatic antioxidant capacity

We next evaluated whether alterations in mitochondria functionality take place in gWAT from UCP3 KO mice. Tissue Cytochrome Oxidase/complex IV activity (COX), a known index of maximal tissue oxidative capacity, was significantly inhibited in KO mice (−19% vs. WT) (Figure 3A). To have indications about an eventual difference in mitochondrial tissue content between WT and KO mice, the levels of the five respiratory complexes both in total tissue and in isolated mitochondria were detected. As reported in Figure 3C, despite any difference in respiratory complexes level in isolated mitochondria, they were significantly enhanced in total tissue lysate from KO mice (Figure 3D), thus indicating an enhancement of mitochondrial tissue content (about doubled in KO mice). Accordingly, specific COX activity, obtained by normalizing tissue COX activity for COX tissue level (i.e., complex IV levels), was further reduced in KO mice compared to WT (−68%) (Figure 3B).

Given the suggested role of UCP3 in mitigating oxidative stress, we also evaluated ROS levels in mitochondrial enriched fraction, and the mitochondrial enzymatic antioxidant capacity (Figure 4). The absence of UCP3 is associated with an increase in mitochondrial ROS abundance (+58% in KO vs. WT ones, Figure 4A). In addition, superoxide dismutase protein-2 (SOD2) and glutathione peroxidase-4 levels were significantly enhanced in KO mice

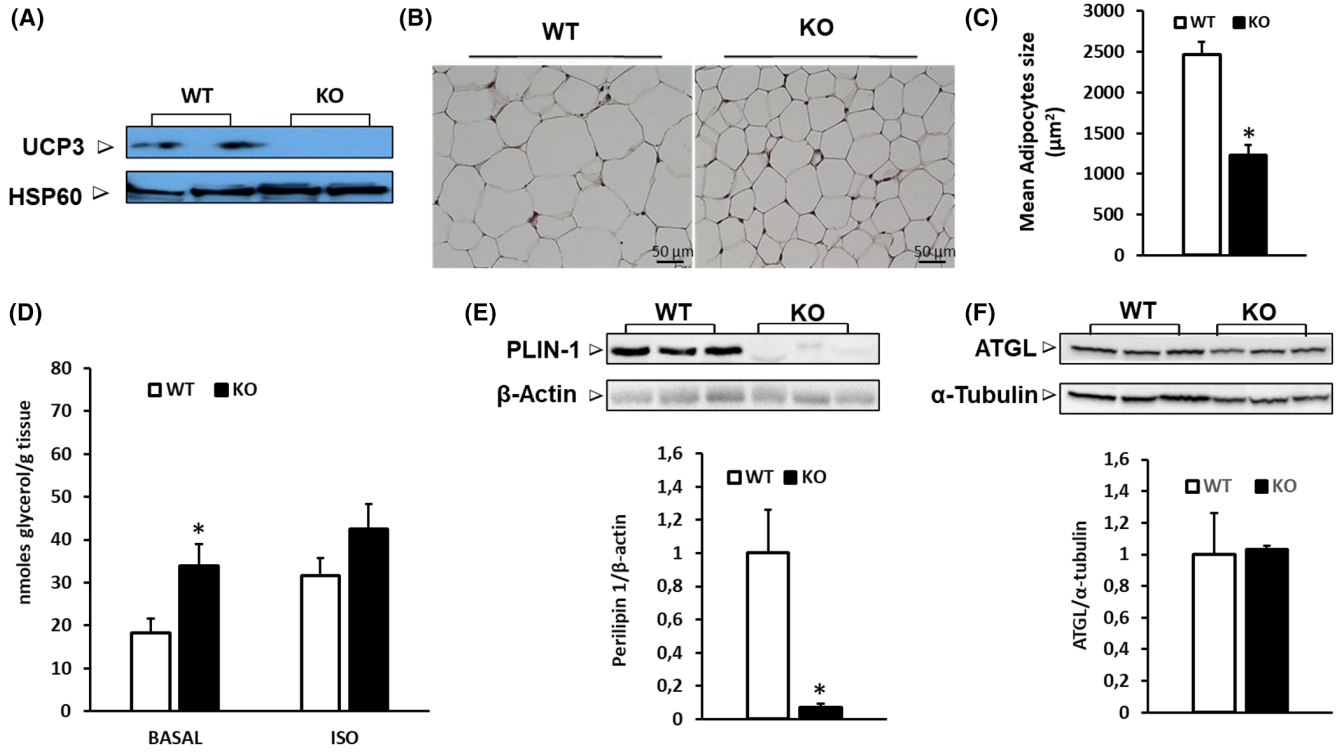

FIGURE 1 UCP3 levels (A), gWAT morphology (B) and adipocytes mean area (C), glycerol release by gWAT (D), and levels of proteins involved in lipolysis (E, F) detected in gWAT from WT and KO mice. Panel A shows a representative western blot of UCP3 levels detected in gWAT isolated mitochondria lysates (30 µg of protein/mouse/lane) from WT and KO mice receiving vehicle or insulin. HSP60 was used as a loading control. Panel B shows representative histological analysis of gWAT from WT and KO mice acclimated at thermoneutrality (30°C) for 4 weeks. Hematoxylin and eosin staining. Values represent the mean ± SE. $n = 3$. Panel D shows glycerol release by gWAT detected in basal conditions and in the presence of isoproterenol (ISO). Panels E and F show a representative Western blot of perilipin 1 (PLIN-1), adipose triglycerides lipase (ATGL) levels detected in gWAT tissue lysates (15 µg of protein/mouse/lane) from WT and KO mice. α-tubulin or β actin were used as the loading controls for total tissue lysates (15 µg of protein/mouse/lane). The relative histograms represent the quantification of signals data. Data were normalized to the value obtained for WT animals, set as 1. Values represent the mean ± SEM of 8 different mice *$p < .01$ versus WT

(+120% and +40% vs. WT, respectively, Figure 4C,D), while the levels of catalase were not affected by the absence of UCP3 (Figure 4B).

3.4 | In gWAT, the absence of UCP3 leads to ER stress

To shed light on the possibility that the absence of UCP3 could be associated with ER stress, we evaluated the level of its specific markers, such as the chaperones GRP78-BIP and Calnexin. In gWAT from KO mice increased levels of the two chaperones were observed (by about six- and two-fold vs. WT control, for GRP78-BIP and calnexin, respectively) (Figure 5A), thus indicating the occurrence of ER stress in KO tissues. In addition, we observed that in KO mice some signaling pathways, associated with ER stress and involved in the reduction of adipocytes' responsivity to insulin, are activated, too.

The Eukaryotic translation initiation factor 2 alpha (eIF2a) is a key component of RNA-dependent protein kinase (PKR)-like ER eukaryotic initiation factor-2 alpha kinase (PERK) associated branch of UPR^{ER}. Although no significant changes in its levels can be observed between WT and KO samples, significantly higher levels of the phosphorylated/active form of the protein as well as an enhanced p-eIF2-α/eIF2-α ratio were detected in the KO mice (by about 7 and 9 fold vs. WT, respectively), thus indicating the activation of the eIF2-α signaling pathway (Figure 5B).

Terminal Kinase (JNK) is known to be activated by inositol-requiring ER-to-nucleus signaling protein 1 (IRE-1) associated UPR^{ER} branch. Total and phosphorylated levels JNK were increased in tissue from KO mice (by about four- and 15- fold vs. WT mice, respectively). The p-JNK/JNK ratio was also enhanced in KO mice (by about three-fold), thus indicating the activation of the kinase (Figure 5C).

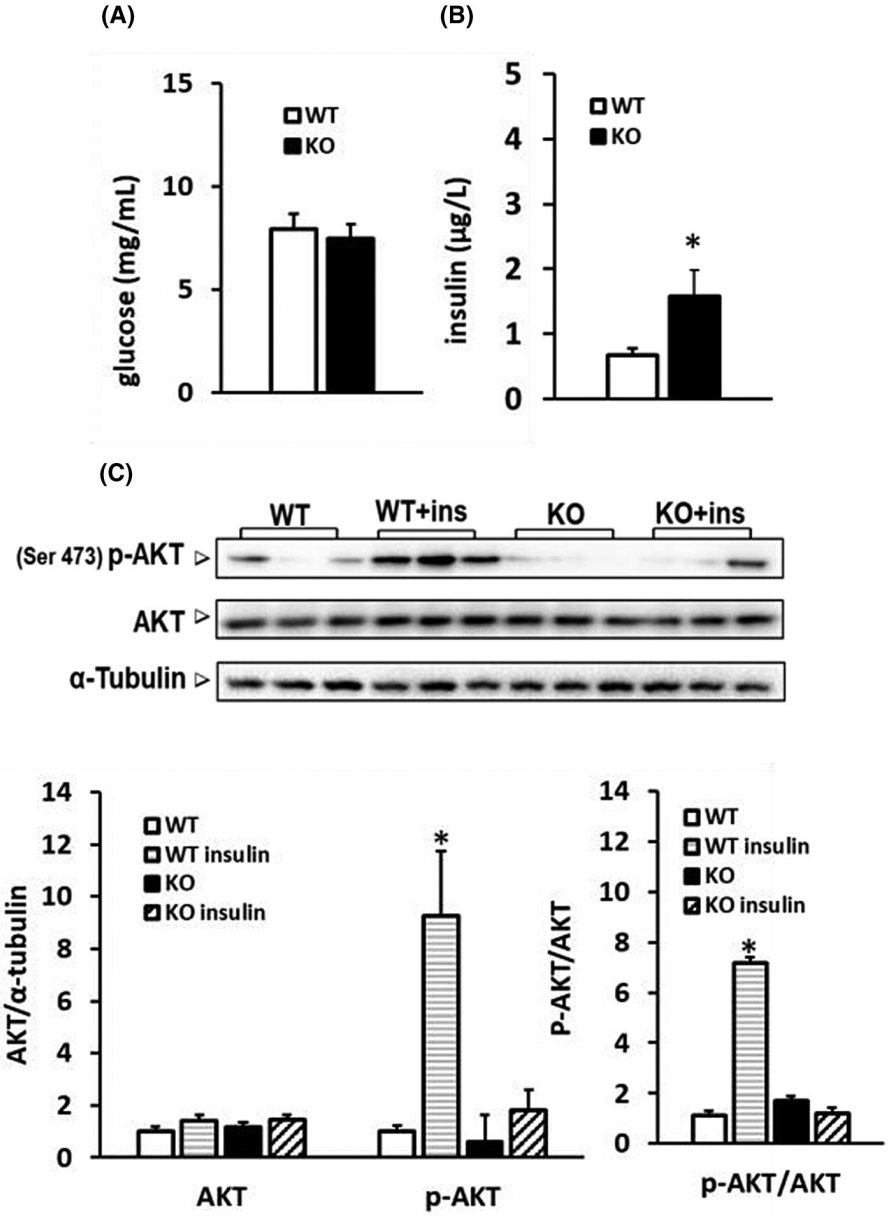

FIGURE 2 Serum levels of glucose (A) and insulin (B) and response to insulin of gWAT from WT and KO mice (C). Representative western blot of total AKT and Ser 473 AKT phosphorylation, detected in gWAT tissue lysates (15 µg of protein/mouse/lane) from WT and KO mice receiving vehicle or insulin. α-tubulin was used as a loading control. The relative histograms represent the quantification of signals data. Data were normalized to the value obtained for WT animals, set as 1. Values represent the mean ± SEM of 8 different mice *$p < .01$ versus WT sham **$p < .01$ versus KO sham and WT ins

3.5 | Absence of UCP3 affects adipokines levels

Next, we performed an adipokines array to evaluate whether the absence of UCP3 could affect adipokines levels in gWAT as well as in sera. In gWAT, Adiponectin and IGFBP1 levels were downregulated in KO mice versus WT ones (−20% and −40% vs. WT, respectively), while DPPIV and Fetuin were significantly increased (+13% and +16%, respectively). (Figure 6). Western blot analysis revealed that chemotactic protein-1 (MCP1) and Tumor Necrosis Factor Alpha (TNF-α) were significantly enhanced in KO mice (four-fold and sevenfold vs. WT, respectively) (Figure 7A,B).

A decrease in adiponectin levels was also observed in KO mice when the adipokines protein array was performed on serum samples (−38% vs. WT). In addition, in sera, we also observed a significant reduction in Endocan, IGFBP-6, and

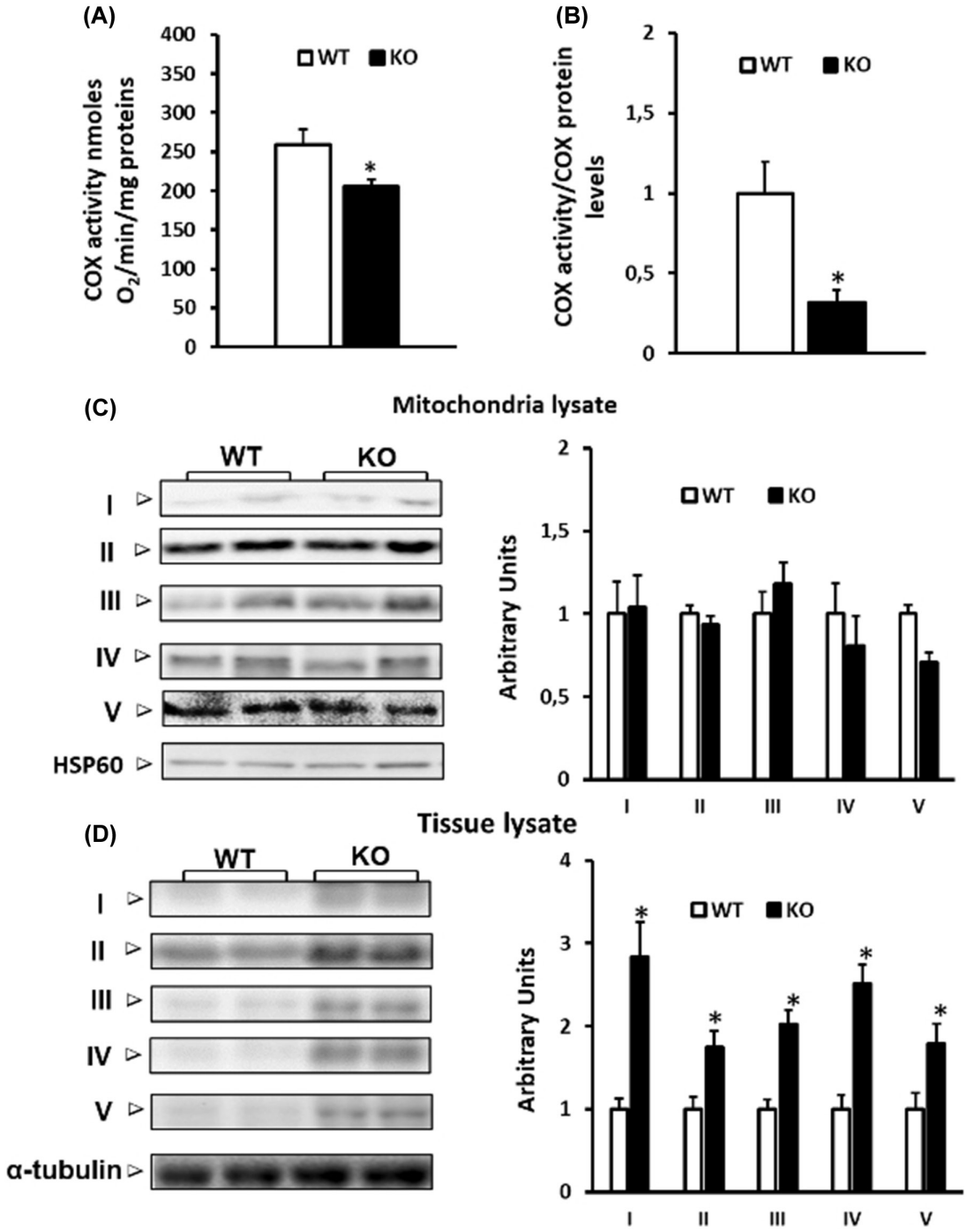

FIGURE 3 Cytochrome oxidase activity and respiratory complexes abundance in gWAT from WT and KO mice. Cytochrome oxidase activity was reported as nmolesO_2/min mg tissue proteins (A) or normalized for tissue COX (also known as Complex IV) levels and expressed in arbitrary units (B). Panels C and D show representative Western blots of CI-NDUF88, CII-SDHB, CIII-UQCRC2, CIV-MTCO1, and CV-ATP VA subunits detected in isolated mitochondria from gWAT and in tissue lysate, respectively. HSP60 and α-tubulin were used as loading controls for mitochondrial lysates (15 μg of protein/mouse/lane) and total tissue lysates (15 μg of protein/mouse/lane), respectively. Histograms represent the quantification of data. Data were normalized to the value obtained for WT animals, set as 1. Values represent the mean ± SEM of 8 different mice

Tissue inhibitor of metalloproteinases-1 (TimP-1) protein levels (−48%, −28%, and −45% vs. WT, respectively) associated with high levels of Serpin E-1, also known as Plasminogen activator inhibitor 1 (PAI-1) (two-fold) (Figure 8).

4 | DISCUSSION

The role of UCP3 in homeostasis is progressively emerging and the present study helps to clarify its importance

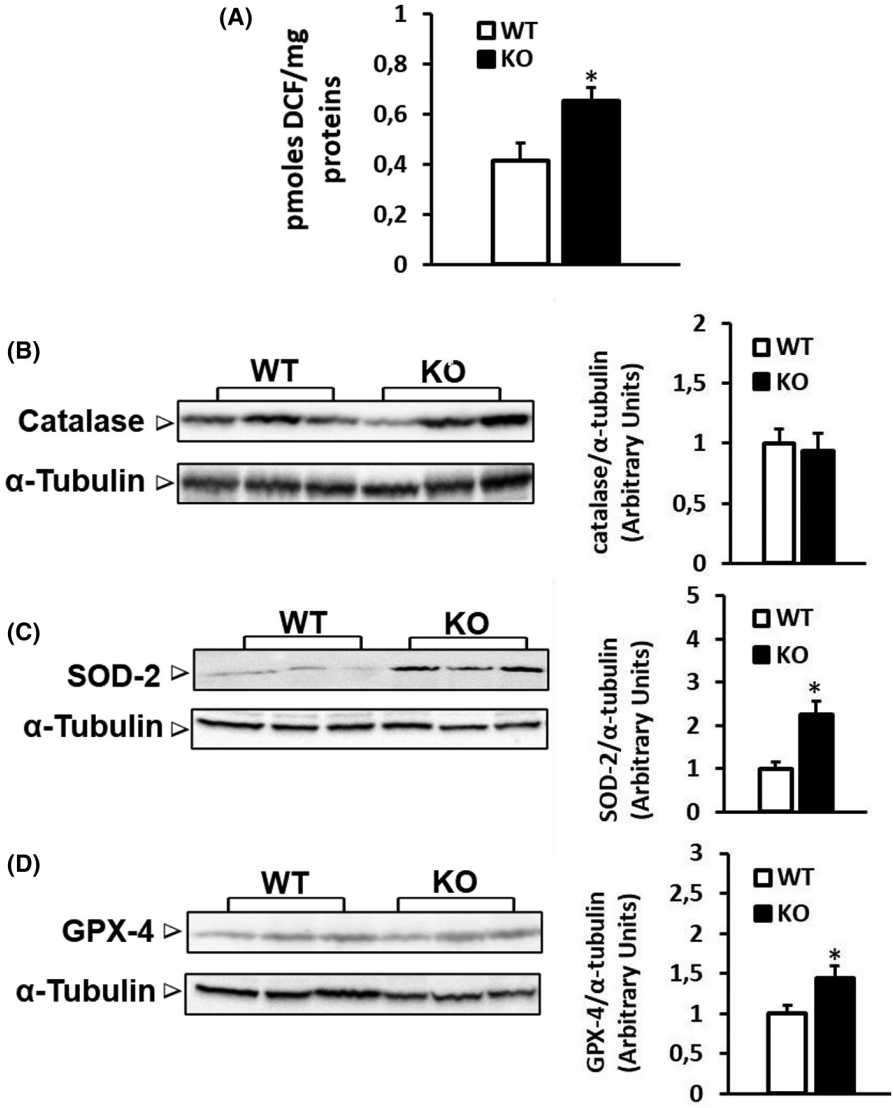

FIGURE 4 Mitochondrial ROS levels (A) and abundance of mitochondrial antioxidant enzymes (B-D) detected in gWAT from WT and KO mice. Panel A ROS content, detected in gWAT isolated mitochondria, by evaluating changes in the DCF oxidation. Panels B-D Representative Western blots of catalase (CAT) (B) superoxide dismutase 2 (SOD-2) (C), and glutathione peroxidase 4 (GPX-4) (D) in gWAT lysate (15 μg of protein/mouse/lane). Histograms represent the quantification of data. Data were normalized to the value obtained for WT animals, set as 1, and represent the mean ± SEM of 8 different mice. *$p < .01$ versus WT

in the functionality of adipose tissue which exerts a significant control on energy metabolism. We report that the absence of UCP3 impacts the capacity of gWAT to store TG, its response to insulin, as well its endocrine functions.

The reduced capacity of KO mice to store TG in gWAT is reflected by the lower contribution of tissue's weight to animal weight, the reduced adipocytes size, and the enhanced lipolysis. PLIN-1, one major lipid droplet binding protein that prevents "attack" of TGs by lipases, whose deficiency in mice is associated with reduced fat mass.[23] In addition, PLIN-1 binds the ATGL co-activator (α/β hydrolase domain-containing protein 5 ABHD5/CGI-58), thus preventing the latter from interacting with and activating ATGL.[24] The dissociation of PLIN-I from the lipid droplet detaches ABHD5/CGI-58 from the same PLIN-1, which allows ATGL activation. In view of the above, the strong reduction of PLIN-1 levels detected in KO mice likely contributes to the enhanced basal lipolysis. Inflammatory processes, mediated by TNF-α, are known to activate lipolysis and to reduce PLIN-1 mRNA and protein expression[25] thus, the increased levels of TNF-α observed in KO mice might contribute to influencing adipose lipolysis via PLIN-1 downregulation, other than influencing insulin sensibility of the tissue (later discussed).

Here, we also report that the absence of UCP3 leads to mitochondrial dysfunction/damage since, even though in KO mice tissue' mitochondrial content was almost doubled, gWAT maximal oxidative capacity was significantly

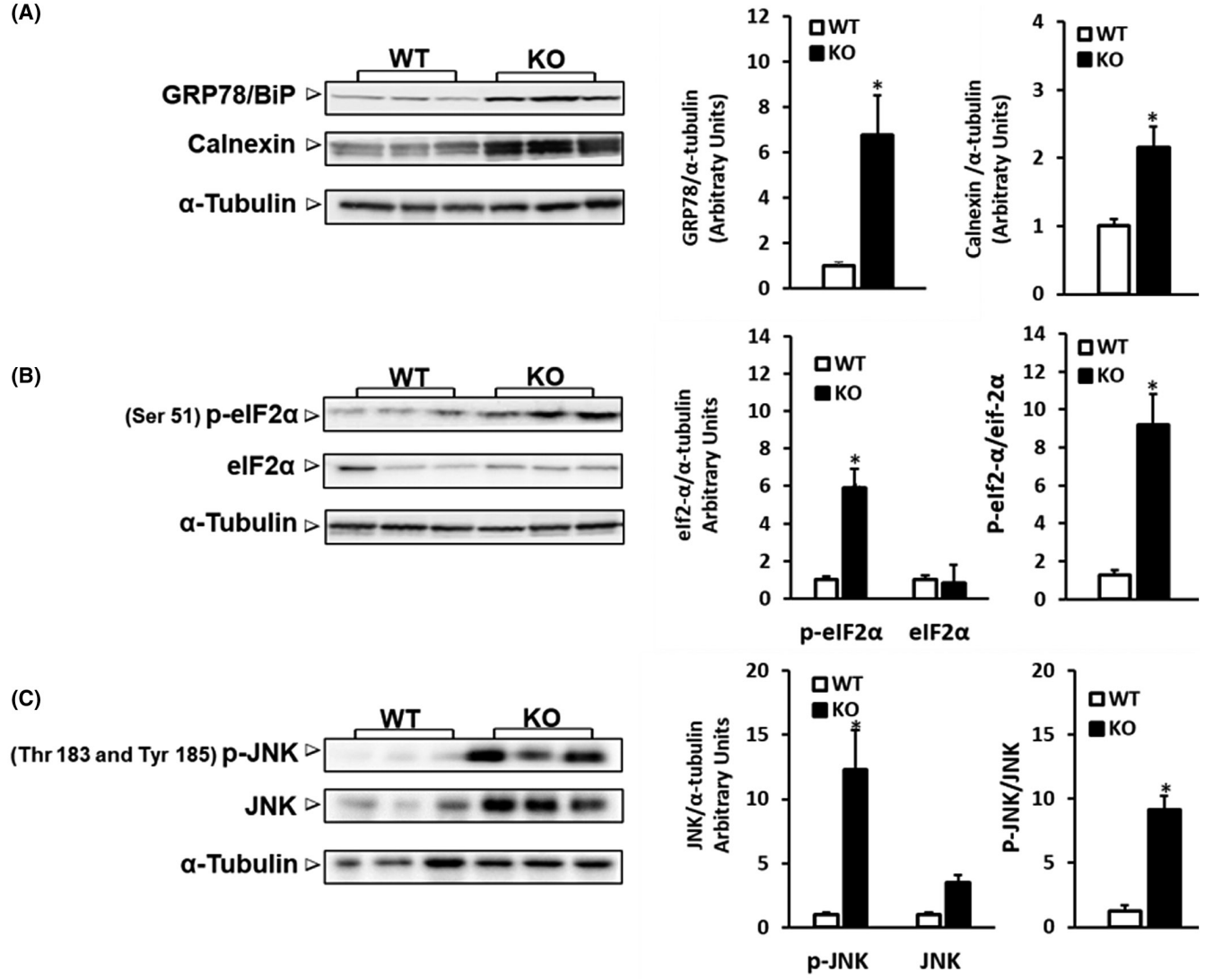

FIGURE 5 Levels of proteins involved in ER stress and UPR^{ER} response detected in gWAT from WT and KO mice. Representative Western blots of GRP78/BIP, Calnexin (A), total and phosphorylated (ser 78) levels of eIF2α (B), and total and phosphorylated levels (Thr 183 tyr 185) of JNK, performed in gWAT lysate (15 μg of protein/mouse/lane). Histograms represent the quantification of data. Data were normalized to the value obtained for WT animals, set as 1, and represent the mean ± SEM of 6–8 different mice. *$p < .01$ versus WT

reduced. The higher ROS levels observed in mitochondria from KO mice as well as the enhancement of SOD-2 and GPX-4, two enzymes involved in the first line antioxidants defense and strategic to protect mitochondria from the damage induced by O_2^-, H_2O_2 and LOOH are in line with the role played by UCP3 in mitigating mitochondrial oxidative stress. The higher mitochondrial ROS content detected in gWAT from KO mice, linked to mitochondrial dysfunction despite an increase in gWAT mitochondria content, implies a failure in mitochondrial quality control.

ER stress is associated with pathologic mitochondrial dysfunction.[13] Our data demonstrate that the absence of UCP3 leads to ER stress, associated with mitochondrial dysfunction, insulin resistance, and inflammation. The mechanism by which ER stress interferes with insulin signaling[25] is multifactorial (for review, see Villalobor-Labra et al.[15]); it seems to involve two different branches of UPR^{ER}, such as IRE1α/JNK, and PERK/eif2α/ATF4 signaling. Concerning the first, following its activation, JNK directly phosphorylates IRS1 and IRS2 at serine and threonine residues, leading to reduced tyrosine-phosphorylation of IRS1/2 molecules and to decreased recruitment of the PI3K-AKT signaling pathway in response to insulin.[26–28] In addition, the activation of PERK/eif2α/ATF4 signaling leads to the expression of a tribbles-like protein 3 (TRB3), a pseudokinase that contrasts insulin-induced Akt activation.[29,30] gWAT from KO mice is insulin resistant, as revealed by the impaired ability of the hormone to induce the activation/phosphorylation of Akt (ser 473). The activation of both eif-2α (ser 51) and the increased levels of the total and phosphorylated form of JNK (Thr83/tyr185), observed in gWAT from KO

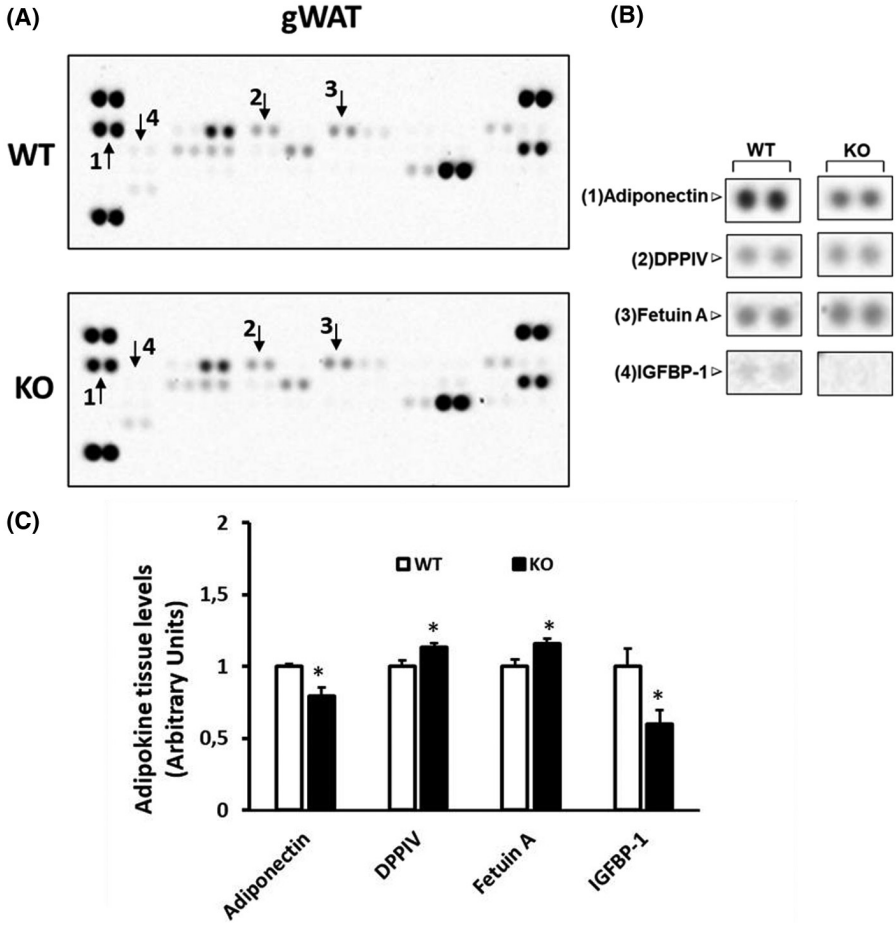

FIGURE 6 Adipokines profiles obtained in gWAT from WT and KO mice. Adipokine profile detected in gWAT from WT and KO mice, by a mouse adipokine protein array (A). The arrowheads indicate signals with significant changes that were then magnified (B). Histograms represent the quantification of relative levels of adipokines with observable changes (C). The values represent the mean ± SEM of 4 different samples, each one obtained by a pool of two different animals. Data were normalized to the value obtained for WT animals, set as 1. *$p < .01$ versus WT

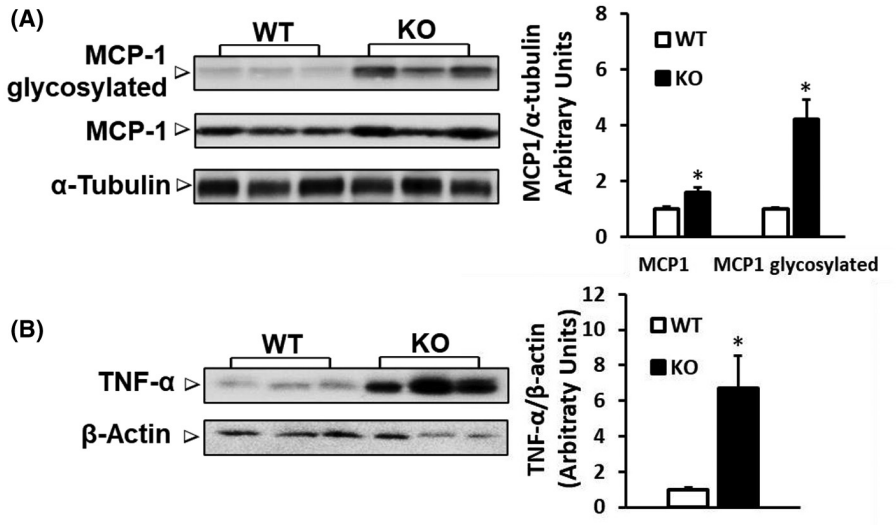

FIGURE 7 MCP1 and TNFα levels detected in gWAT from WT and KO mice. Representative Western blots of MCP1 (A) and TNF-α (B) in gWAT lysates (15 μg of protein/mouse/lane) detected in gWAT lysates. Histograms represent the quantification of data. Data were normalized to the value obtained for WT animals, set as 1, and represent the mean ± SEM of 8 different mice. *$p < .01$ versus WT

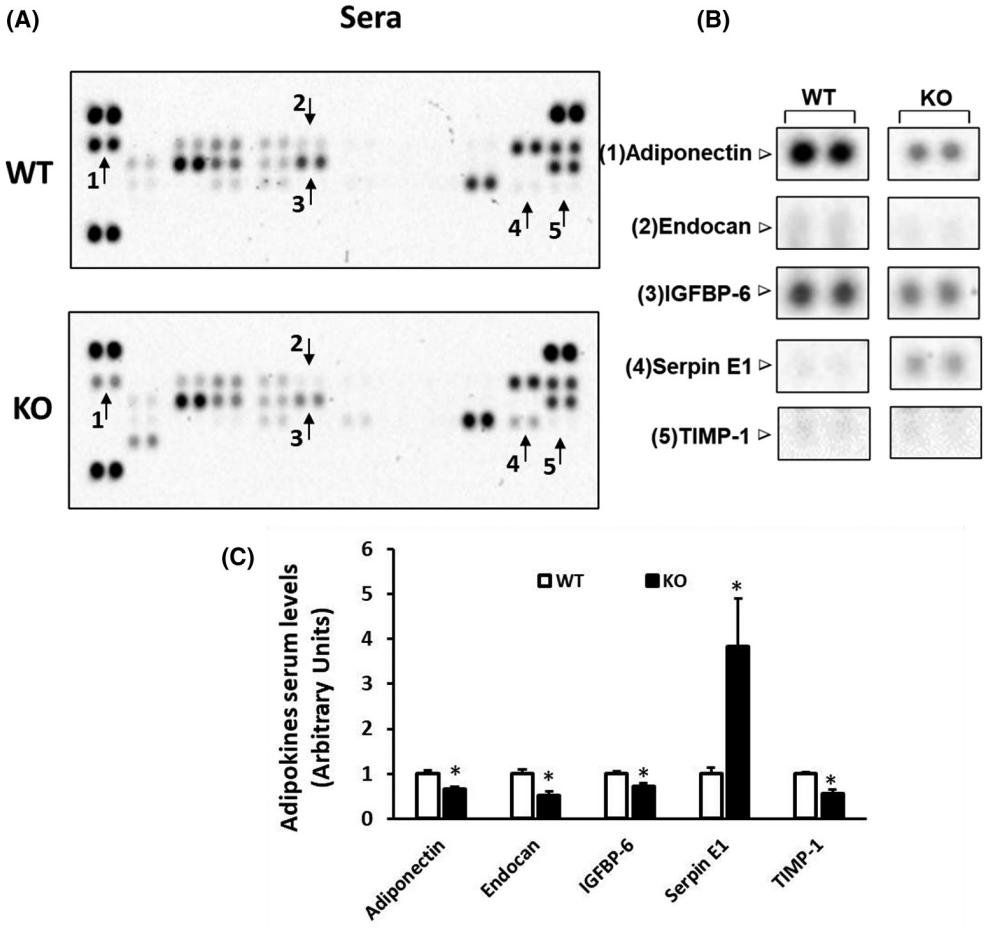

FIGURE 8 Adipokines profiles obtained in sera from WT and KO mice. Adipokine profile detected in sera from WT and KO mice, by a mouse adipokine protein array (A). The arrowheads indicate signals with significant changes that were then magnified (B). Histograms represent the quantification of relative levels of adipokines with observable changes (C). The values represent the mean ± SEM of 4 different samples, each one obtained by a pool of two different animals. Data were normalized to the value obtained for WT animals, set as 1. *$p < .01$ versus WT

mice, likely underly the reduction of the responsivity of gWAT to insulin. However, it is important to highlight that both eif2α and JNK are considered "stress proteins", thus it is possible that signaling pathways, other than that directly involved in UPR^{ER}, could have participated in their activation. In addition to insulin resistance, ER stress is also closely associated with inflammation.[31,32]

gWAT from KO mice has increased levels of monocyte chemoattractant protein 1 (MCP-1), known to induce the recruitment of monocytes and to activate proinflammatory macrophages, which in turn release inflammatory proteins. Among these, TNF-α was significantly increased in KO mice, likely contributing to blunting insulin signaling, and in enhancing lipolysis.[33,34]

FFA released by lipolytic adipocytes may also activate TLR4 (present both on macrophages and adipocytes) and then chemokines and cytokines release, thus amplifying insulin resistance, lipolysis, and inflammation.[16] The activation of TLR4 4 by FFA, indeed requires the adipokine Fetuin-A, an endogenous presenter of FFAs to TLR4 to promote lipid-induced insulin resistance[35,36] as well as a key player in reducing adiponectin transcription as well their circulating levels.[37] By means of adipokines array, we reported that gWAT from KO mice displayed enhanced levels of Fetuin-A, thus suggesting its contribution to insulin resistance and inflammation observed in that tissue. Interestingly, it has been reported that in adipocytes Feutin A and adiponectin levels are changed following the induction of ER stress,[38,39] and that TNF- α is able to inhibit adiponectin gene expression and secretion from 3T3-L1 adipocytes.[40] Thus, our data suggest that the occurrence of ER stress in gWAT from KO mice and the consequent inflammation could have been involved in changing the levels of the two adipokines.

By adipokine protein array we also observed that in gWAT the absence of UCP3 is associated with an enhancement of Dipeptidyl peptidase-4 (DPPIV) and a decrease in IGF-binding protein-1 (IGFBP-1), two proteins that can modulate the availability of signaling molecules for the

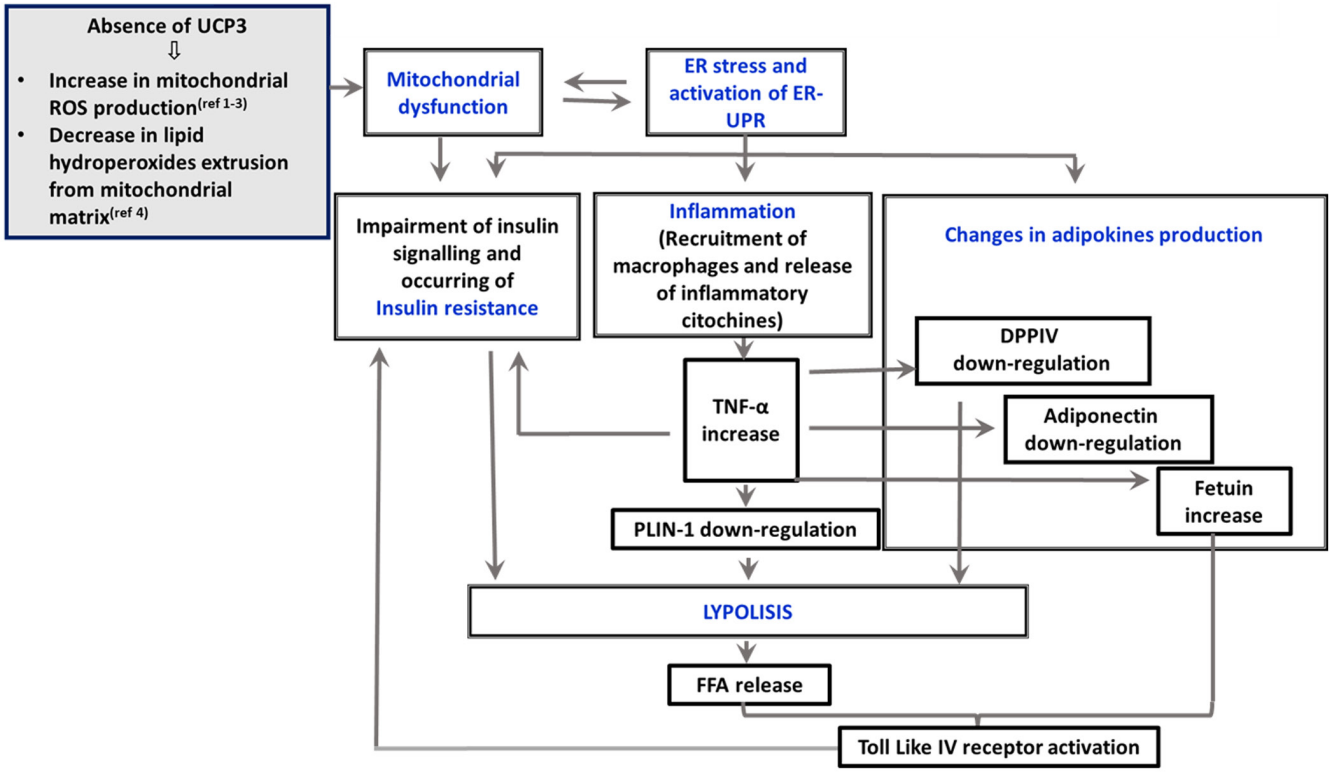

FIGURE 9 The schema represents the interrelated processes occurring in gWAT from KO mice that lead to insulin resistance, lipolysis, and reduced ability of the tissue to store lipids. The grey box indicates that the processes described in it are not directly assayed and refer to the functions attributed to UCP3 reported in literature

adipocytes. DPPIV, also known as adenosine deaminase binding protein, in WAT may have multiple autocrine and paracrine functional implications for the tissue's physiology and resistance to insulin, since (i) it interacts and recruits adenosine deaminase to the cell surface, thus modulating the well-known antilipolytic effects exerted by adenosine on adipocyte[33,41] and its (ii) it cleaves neuropeptide Y, thus reducing its antilipolytic action on adipose tissue[42] and (iii) it directly impairs insulin signaling in adipocytes in vitro.[43] Thus, the increased levels of DPPIV in gWAT from KO mice could have plausibly contributed to enhanced lipolysis as well to the occurrence of insulin resistance. Reasonably the high level of TNF-α, detected in samples from KO mice, could have been responsible for the upregulation of DPPIV.[43] In addition to the above adipokines, adiponectin, an adipose-tissue-derived hormone, plays an important role in the regulation of lipid metabolism and insulin sensitivity and also possesses anti-inflammatory effects[44–46] being considered as an antiatherogenic adipokine.[45] In sera from KO mice, the reduced adiponectin levels are in line with alteration in fatty acids and glucose metabolism, previously reported for these mice[6–9] and with data obtained in human.[47] The changes in PAI-1 and TIMP-1 levels (that are known to be oppositely regulated by adiponectin[48] and that are involved in the formation, progression, and stabilization of atherosclerotic plaques,[49,50] associated with reduced adiponectin levels might support occurrence or atherogenesis.

Interestingly, in gWAT from KO mice, some mechanisms tending to contrast insulin resistance seem to be activated, too. Indeed, the local down-regulation of IGFBP-1 observed in gWAT from KO mice, that would increase the availability and the effect of IGF-1, could be considered a compensatory mechanism, finalized to minimize gWAT insulin resistance and the associated derangements. It is well known that IGF-1 affects adipocyte metabolism and that its activity is acutely regulated by the binding to IGF-binding protein-1 (IGFBP-1). In vitro studies indicate that IGF-1 and IGF-2 are equipotent with insulin in regulating adipocyte metabolism, in terms of stimulation of cell glucose uptake and lipolysis inhibition[43] and that the effects of IGF1 are blunted in the presence of IGFBP-1.[51]

5 | CONCLUSIONS

As a whole major advances have been made in the understanding of the physiological role of UCP3 through the analysis of genetically modified animal models. We show that UCP3 contributes to gWAT insulin sensitivity by influencing mitochondrial and ER compartments in the regulation of inflammatory and lipid metabolism-related pathways.

In KO mice, the occurrence of multifactorial processes interrelated and influencing each other, such as impaired mitochondrial functionality, ER stress, insulin resistance and inflammation, underlie the reduced ability of gWAT to store lipids (Figure 9), but at the moment it is not possible to define univocally which of the listed processes was established first. However, when considering the role proposed by UCP3 in protecting mitochondria from oxidative stress (i.e., mitigation of ROS production by mild uncoupling[2,3] and extrusion of lipid hydroperoxides from mitochondrial matrix[4]), we speculate that the absence of UCP3 first leads to mitochondrial dysfunction; this will induce the other mentioned interrelated processes (Figure 9). It is important to underly that, since we employed whole body UCP3 KO mice, we cannot exclude some other factors related to the absence of UCP3 in tissues expressing the protein other than WAT (i.e., heart, brown adipose tissue, skeletal muscle) could have contributed to influence WAT functionality in our model. Further investigation of the molecular role of UCP3 in gWAT is an important task for the future and may provide new insights into its function in energy homeostasis.

ACKNOWLEDGMENTS

This study was funded by Department of Biology University of Naples Federico II (AL), University of Sannio (MM), and University of Urbino (RdM) Open Access Funding provided by Universita degli Studi di Napoli Federico II within the CRUI-CARE Agreement. [Correction added on June 13, 2022, after first online publication: CRUI-CARE Funding statement has been added.]

DISCLOSURES

The authors declare no conflict of interest.

AUTHOR CONTRIBUTIONS

All authors contributed to the study conception and design and interpretation of data. Alessandra Gentile, Nunzia Magnacca, Rita de Matteis, Antonia Giacco, Rosalba Senese, Federica Cioffi contributed to the acquisition of data. Alessandra Gentile, Nunzia Magnacca, Rita de Matteis, Moreno Maria, Antonia Lanni, Pieter de Lange, Rosalba Senese, Goglia Fernando, Elena Silvestri, Assunta Lombardi drafted the work or revised it critically for important intellectual content; All authors read and approved the final manuscript.

DATA AVAILABILITY STATEMENT

The data that support the findings of this study are already included in the article.

REFERENCES

1. Hilse KE, Kalinovich AV, Rupprecht A, et al. The expression of UCP3 directly correlates to UCP1 abundance in brown adipose tissue. *Biochim Biophys Acta*. 2016;1857(1):72-78.
2. Cioffi F, Senese R, de Lange P, Goglia F, Lanni A, Lombardi A. Uncoupling proteins: a complex journey to function discovery. *BioFactors*. 2009;35(5):417-428.
3. Cadenas S. Mitochondrial uncoupling, ROS generation, and cardioprotection. *Biochim Biophys Acta Bioenerg*. 2018;1859(9):940-950.
4. Lombardi A, Busiello RA, Napolitano L, et al. UCP3 translocates lipid hydroperoxide and mediates lipid hydroperoxide-dependent mitochondrial uncoupling. *J Biol Chem*. 2010;285(22):16599-16605.
5. Silvestri E, Senese R, De Matteis R, et al. Absence of uncoupling protein 3 at thermoneutrality influences brown adipose tissue mitochondrial functionality in mice. *FASEB J*. 2020;34(11):15146-15163.
6. Lombardi A, Busiello RA, De Matteis R, et al. Goglia F absence of uncoupling protein-3 at thermoneutrality impacts lipid handling and energy homeostasis in mice. *Cells*. 2019;8(8):916.
7. Senese R, Valli V, Moreno M, et al. Uncoupling protein 3 expression levels influence insulin sensitivity, fatty acid oxidation, and related signaling pathways. *Pflugers Arch*. 2011;461(1):153-164.
8. Choi CS, Fillmore JJ, Kim JK, et al. Overexpression of uncoupling protein 3 in skeletal muscle protects against fat-induced insulin resistance. *J Clin Invest*. 2007;117(7):1995-2003.
9. Chan CB, Harper ME. Uncoupling proteins: role in insulin resistance and insulin insufficiency. *Curr Diabetes Rev*. 2006;2(3):271-283.
10. Costford SR, Chaudhry SN, Crawford SA, Salkhordeh M, Harper ME. Long-term high-fat feeding induces greater fat storage in mice lacking UCP3. *Am J Physiol Endocrinol Metab*. 2008;295(5):E1018-E1024.
11. Schrauwen P, Hesselink MKC. Oxidative capacity, lipotoxicity, and mitochondrial damage in type 2 diabetes. *Diabetes*. 2000;453(6):1412-1417.
12. Mensink M, Hesselink MK, Borghouts LB, et al. Skeletal muscle uncoupling protein-3 restores upon intervention in the prediabetic and diabetic state: implications for diabetes pathogenesis? *Diabetes Obes Metab*. 2007;9(4):594-596.
13. Lim JH, Lee HJ, Ho Jung M, Song J. Coupling mitochondrial dysfunction to endoplasmic reticulum stress response: a molecular mechanism leading to hepatic insulin resistance. *Cell Signal*. 2009;21(1):169-177.
14. Wang CH, Wang CC, Huang HC, Wei YH. Mitochondrial dysfunction leads to impairment of insulin sensitivity and adiponectin secretion in adipocytes. *FEBS J*. 2013;280(4):1039-1050.
15. Villalobos-Labra R, Subiabre M, Toledo F, Pardo F, Sobrevia L. Endoplasmic reticulum stress and development of insulin resistance in adipose, skeletal, liver, and foetoplacental tissue in diabesity. *Mol Aspects Med*. 2019;66:49-61.
16. Lionetti L, Mollica MP, Lombardi A, Cavaliere G, Gifuni G, Barletta A. From chronic overnutrition to insulin resistance: the role of fat-storing capacity and inflammation. *Nutr Metab Cardiovasc Dis*. 2009;19(2):146-152.
17. Després JP, Lemieux I. Abdominal obesity and metabolic syndrome. *Nature*. 2006;444(7121):881-887.
18. Bjørndal B, Burri L, Staalesen V, Skorve J, Berge RK. Different adipose depots: their role in the development of metabolic syndrome and mitochondrial response to hypolipidemic agents. *J Obes*. 2011;2011:490650.
19. Gong DW, Monemdjou S, Gavrilova O, et al. Lack of obesity and normal response to fasting and thyroid hormone in mice lacking uncoupling protein-3. *J Biol Chem*. 2000;275(21):16251-16257.

20. Clark AM, Sousa KM, Jennings C, MacDougald OA, Kennedy RT. Continuous-flow enzyme assay on a microfluidic chip for monitoring glycerol secretion from cultured adipocytes. *Anal Chem*. 2009;81(6):2350-2356.
21. Lombardi A, Senese R, De Matteis R, et al. 3,5-Diiodo-L-thyronine activates brown adipose tissue thermogenesis in hypothyroid rats. *PLoS One*. 2015;10(2):e0116498.
22. Driver AS, Kodavanti PR, Mundy WR. Age-related changes in reactive oxygen species production in rat brain homogenates. *Neurotoxicol Teratol*. 2000;22(2):175-181.
23. Sohn JH, Lee YK, Han JS, et al. Perilipin 1 (Plin1) deficiency promotes inflammatory responses in lean adipose tissue through lipid dysregulation. *J Biol Chem*. 2018;293(36):13974-13988.
24. Girousse A, Langin D. Adipocyte lipases and lipid droplet-associated proteins: insight from transgenic mouse models. *Int J Obes*. 2012;36:581-594.
25. Rydén M, Arvidsson E, Blomqvist L, Perbeck L, Dicker A, Arner P. Targets for TNF-alpha-induced lipolysis in human adipocytes. *Biochem Biophys Res Commun*. 2004;318(1):168-175.
26. Ozcan U, Cao Q, Yilmaz E, et al. Endoplasmic reticulum stress links obesity, insulin action, and type 2 diabetes. *Science*. 2004;306(5695):457-461.
27. Xu L, Spinas GA, Niessen M. ER stress in adipocytes inhibits insulin signaling, represses lipolysis, and alters the secretion of adipokines without inhibiting glucose transport. *Horm Metab Res*. 2010;42(9):643-651.
28. Flamment M, Hajduch E, Ferré P, Foufelle F. New insights into ER stress-induced insulin resistance. *Trends Endocrinol Metab*. 2012;23(8):381-390.
29. Du K, Herzig S, Kulkarni RN, Montminy M. TRB3: a tribbles homolog that inhibits Akt/PKB activation by insulin in liver. *Science*. 2003;300(5625):1574-1577.
30. Ozcan L, Cristina de Souza J, Harari AA, Backs J, Olson EN, Tabas I. Activation of calcium/calmodulin-dependent protein kinase II in obesity mediates suppression of hepatic insulin signaling. *Cell Metab*. 2013;18(6):803-815.
31. Gregor MF, Hotamisligil GS. Thematic review series: Adipocyte Biology. Adipocyte stress: the endoplasmic reticulum and metabolic disease. *J Lipid Res*. 2007;48(9):1905-1914.
32. Foley KP, Chen Y, Barra NG, et al. Inflammation promotes adipocyte lipolysis via IRE1 kinase. *J Biol Chem*. 2021;296:100440.
33. Frühbeck G, Méndez-Giménez L, Fernández-Formoso JA, Fernández S, Rodríguez A. Regulation of adipocyte lipolysis. *Nutr Res Rev*. 2014;27(1):63-93.
34. Hotamisligil GS. Molecular mechanisms of insulin resistance and the role of the adipocyte. *Int J Obes Relat Metab Disord*. 2000;24(Suppl 4):S23-S27.
35. Pal D, Dasgupta S, Kundu R, et al. Fetuin-A acts as an endogenous ligand of TLR4 to promote lipid-induced insulin resistance. *Nat Med*. 2012;18(8):1279-1285.
36. Dasgupta S, Bhattacharya S, Biswas A, et al. NF-kappaB mediates lipid-induced fetuin-A expression in hepatocytes that impairs adipocyte function effecting the insulin resistance. *Biochem J*. 2010;429(3):451-462.
37. Agarwal S, Chattopadhyay M, Mukherjee S, Dasgupta S, Mukhopadhyay S, Bhattacharya S. Fetuin-A downregulates adiponectin through Wnt-PPARγ pathway in lipid induced inflamed adipocyte. *Biochim Biophys Acta Mol Basis Dis*. 2017;1863(1):174-181.
38. Mondal AK, Das SK, Varma V, et al. Effect of endoplasmic reticulum stress on inflammation and adiponectin regulation in human adipocytes. *Metab Syndr Relat Disord*. 2012;10(4):297-306.
39. Torre-Villalvazo I, Bunt AE, Alemán G, et al. Adiponectin synthesis and secretion by subcutaneous adipose tissue is impaired during obesity by endoplasmic reticulum stress. *J Cell Biochem*. 2018;119(7):5970-5984.
40. Fasshauer M, Klein J, Neumann S, Eszlinger M, Paschke R. Hormonal regulation of adiponectin gene expression in 3T3-L1 adipocytes. *Biochem Biophys Res Commun*. 2002;290(3):1084-1089.
41. Fredholm BB. Adenosine and lipolysis. *Int J Obes*. 1981;5(6):643-649.
42. Kos K, Baker AR, Jernas M, et al. DPP-IV inhibition enhances the antilipolytic action of NPY in human adipose tissue. *Diabetes Obes Metab*. 2009;11(4):285-292.
43. Lamers D, Famulla S, Wronkowitz N, et al. Dipeptidyl peptidase 4 is a novel adipokine potentially linking obesity to the metabolic syndrome. *Diabetes*. 2011;60(7):1917-1925.
44. Yamauchi T, Kamon J, Waki H, et al. The fat-derived hormone adiponectin reverses insulin resistance associated with both lipoatrophy and obesity. *Nat Med*. 2001;7(8):941-946.
45. Yamauchi T, Hara K, Kubota N, et al. Dual roles of adiponectin/Acrp30 in vivo as an anti-diabetic and anti-atherogenic adipokine. *Curr Drug Targets Immune Endocr Metabol Disord*. 2003;3(4):243-254.
46. Antoniades C, Antonopoulos AS, Tousoulis D, Stefanadis C. Adiponectin: from obesity to cardiovascular disease. *Obes Rev*. 2009;10(3):269-279.
47. De Luis Roman DA, Aller R, Izaola Jauregui O, et al. Relation of -55CT polymorphism of uncoupling protein 3 gene with fat mass and insulin resistance in morbidly obese patients. *Metabolism*. 2010;59(4):608-612.
48. Ramezani-Moghadam M, Wang J, Ho V, et al. Adiponectin reduces hepatic stellate cell migration by promoting tissue inhibitor of metalloproteinase-1 (TIMP-1) secretion. *J Biol Chem*. 2015;290(9):5533-5542.
49. Sobel BE. Increased plasminogen activator inhibitor-1 and vasculopathy. A reconcilable paradox. *Circulation*. 1999;99(19):2496-2498.
50. de Vries MR, Niessen HW, Löwik CW, Hamming JF, Jukema JW, Quax PH. Plaque rupture complications in murine atherosclerotic vein grafts can be prevented by TIMP-1 overexpression. *PLoS One*. 2012;7(10):e47134.
51. Siddals KW, Westwood M, Gibson JM, White A. IGF-binding protein-1 inhibits IGF effects on adipocyte function: implications for insulin-like actions at the adipocyte. *J Endocrinol*. 2002;174(2):289-297.

How to cite this article: Gentile A, Magnacca N, de Matteis R, et al. Ablation of uncoupling protein 3 affects interrelated factors leading to lipolysis and insulin resistance in visceral white adipose tissue. *FASEB J*. 2022;36:e22325. doi:10.1096/fj.202101816RR